Supplementary Information

S1 Fractional cover of JULES PFTs

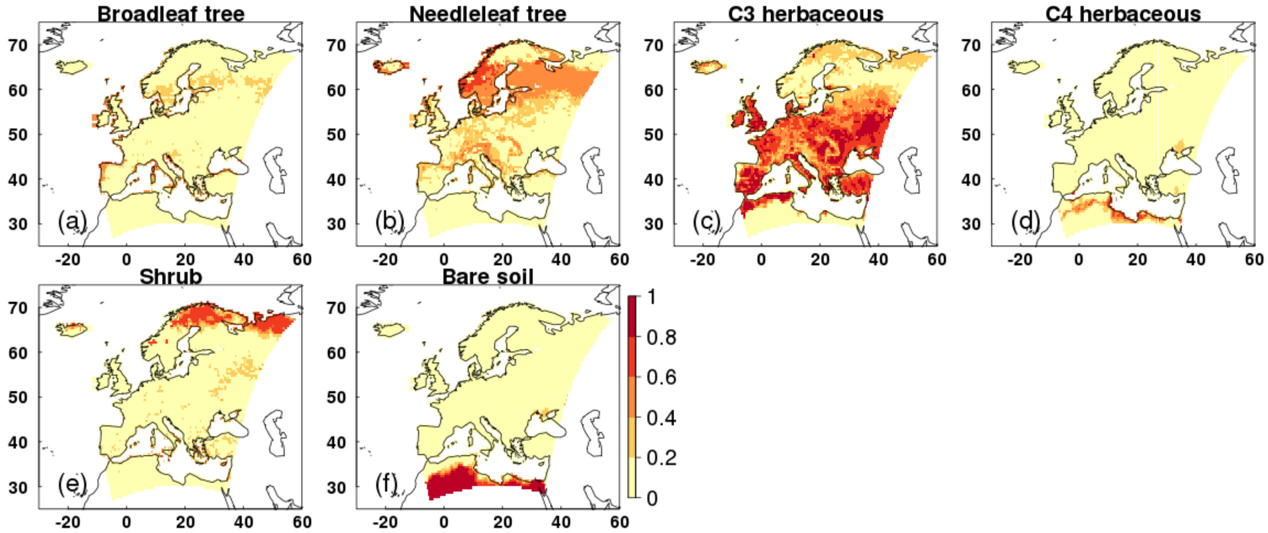

Figure S1. Fractional cover of each JULES PFT and bare soil at 0.5° x 0.5° resolution.

S2 Calibration of O_3 uptake model for European vegetation

Here we use the latest literature on O_3 dose-response relationships derived from observed field data across Europe (CLRTAP, 2017) to calculate the key PFT-specific parameters. Data comes from the UNECE CLRTAP (2017) report which is a synthesis of the latest peer reviewed literature, collated by a panel of experts and so is considered the state-of the art knowledge. Each PFT was calibrated for a high and low plant O_3 sensitivity to account for uncertainty in the sensitivity of different plant species to O_3, using the approach of Sitch *et al*., (2007). In addition, where possible owing to available data, a distinction was made for Mediterranean regions. This was because the work of Büker et al. (2015) showed that different O_3 dose-response relationships are needed to describe the O_3 sensitivity of dominant Mediterranean trees. For the C_3 herbaceous PFT – the dominant land cover type across the European domain in this study (Fig. S1) - the O_3 sensitivity was calibrated against observations for wheat to give a representation of agricultural regions (high plant O_3 sensitivity), versus natural grassland (low plant O_3 sensitivity), with a separate function for Mediterranean grasslands (low plant O_3 sensitivity), all taken from CLRTAP (2017). Tree/shrub PFTs were calibrated against observed O_3 dose-response functions for the high plant O_3 sensitivity (BT = Birch/Beech, BT-Med = deciduous oaks, NT = Norway spruce, shrub = Birch/Beech) all from CLRTAP (2017). The low plant O_3 sensitivity functions for trees/shrubs were calibrated as being 20 % less sensitive based on the difference in sensitivity between high and low sensitive tree species in the Karlsson et al. (2007) study. Due to limitations in data availability, the shrub parameterisation uses the observed dose-response functions for broadleaf trees. Similarly, the parameterisation for C_4 herbaceous uses the observed dose-responses for C_3 herbaceous, however the fractional cover of C_4 herbs across Europe is low (Fig. S1), so this assumption affects a very small percentage of land cover. See Table S1 and Figure S2.

To calibrate the O_3 uptake model for the fast carbon fluxes, e.g. net primary productivity (NPP), JULES was run across Europe forced using the WFDEI observational climate dataset (Weedon, 2013) at 0.5° X 0.5° spatial and three hour temporal resolution. JULES uses interpolation to disaggregate the forcing data down from 3 hours to an hourly model time step. The model was spun-up over the period 1979 to 1999 with a fixed atmospheric CO_2 concentration of 368.33 ppm (1999 value from Mauna Loa observations, (Tans and Keeling)). Zero tropospheric ozone concentration was assumed for the control simulation, for the simulations with O_3, spin-up used spatially explicit fields of present day O_3 concentration produced using the UK Chemistry and Aerosol (UKCA) model with standard chemistry from the run evaluated by O'Connor et al. (2014). A fixed land cover map was used based on IGBP (International Geosphere-Biosphere Programme) land cover classes (IGBP-DIS), therefore as the vegetation distribution was fixed and the calibration was not looking at carbon stores, a short spin-up was adequate to equilibrate soil temperature and soil moisture. JULES was then run for year 2000 with a corresponding CO_2 concentration of 369.52 ppm (from Mauna Loa observations, (Tans and Keeling)) and monthly fields of spatially explicit tropospheric O_3 (O'Connor et al., 2014) as necessary.

Calibration was performed using four simulations: with i) zero tropospheric O_3 concentration, this was the control simulation (NPP_control), ii) tropospheric O_3 at current ambient concentration (NPP_O3), iii) ambient +20 ppb (NPP_O3+20) and iv) ambient +40 ppb (NPP_O3+40). The different O_3 simulations (i.e. ambient, ambient + 20 and ambient + 40 ppb) were used to capture the range of O_3 conditions used in constructing the observed O_3 dose-response relationships deployed for calibration, often these had been constructed under artificially manipulated conditions of ambient + 40 ppb O_3 for example. For each simulation with O_3, JULES used the observed PFT-specific threshold value of O_3 uptake (i.e. parameter F_{O3crit}), and an initial estimate of the parameter 'a' (equation 2). For each PFT and each simulation, hourly estimates of NPP and O_3 uptake for the top sunlit leaf in excess of F_{O3crit} were accumulated over a PFT dependent accumulation (i.e. ~6 months for broadleaf trees and shrubs, all year for needle leaf trees, and ~3 months for herbaceous species, through the growing season). Change in total NPP over the accumulation period (NPP_O3/+20/+40 divided by NPP_control) was calculated for each O_3 simulation and plotted against the cumulative uptake of O_3 over the same period. The linear regression of this relationship was calculated, and slope and intercept compared against the observed dose-response relationships. Values of the parameter 'a' were adjusted, and the procedure repeated until the linear regression through the simulation points matched that of the observations (Fig. S2). JULES is run to be as comparable as possible to the dose-based O_3 risk indicator used in CLRTAP (2017), as only the O_3 flux to top of canopy sunlit leaves is accumulated (i.e. the O_3 flux per projected leaf area). See Table S1 Figure S2.

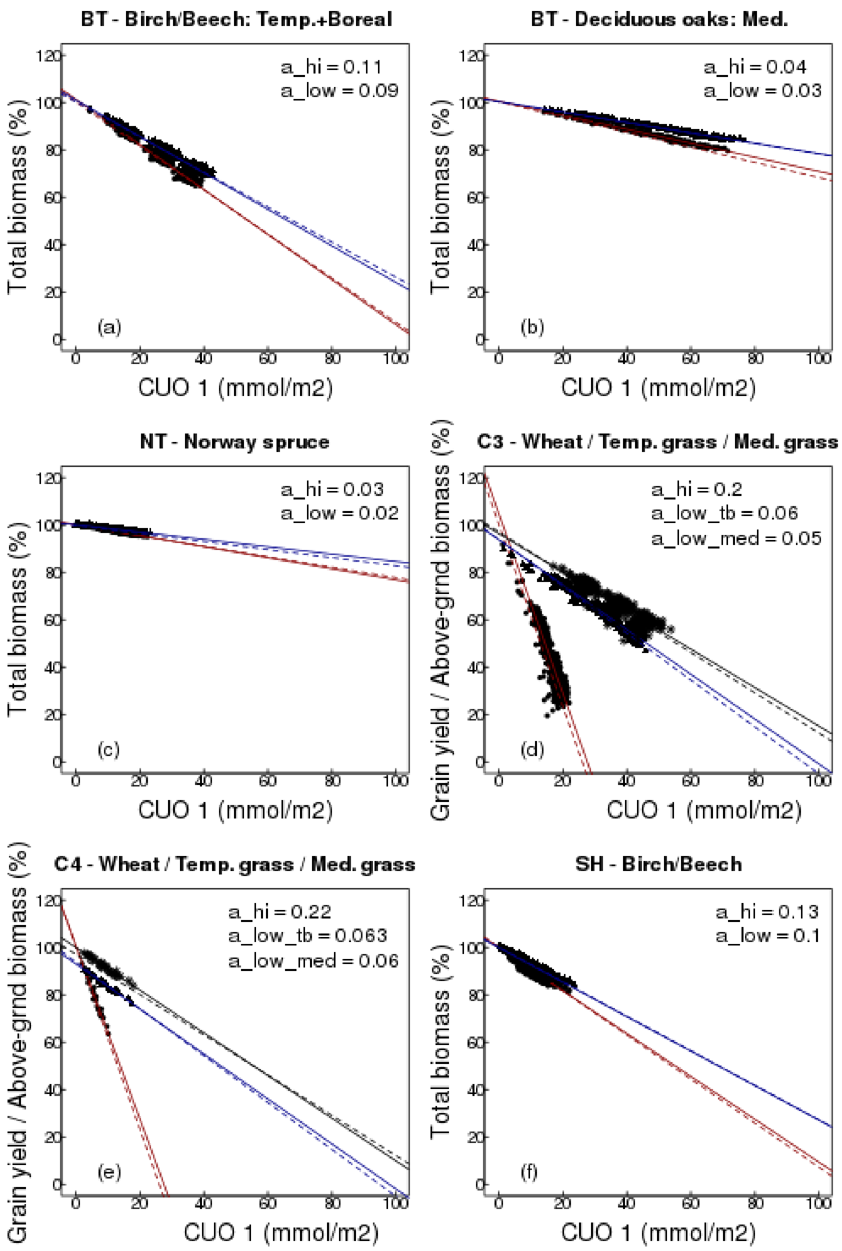

Figure S2. Calibration of JULES for O_3 impacts on plant productivity for each JULES PFT ; a) broadleaf tree – temperate/boreal, b) broadleaf tree Mediterranean, c) Needle leaf tree, d) C_3 herbaceous (split into temperate/boreal and Mediterranean for the natural grasslands), e) C_4 herbaceous (split into temperate/boreal and Mediterranean for the natural grasslands), and f) shrub. High (red) and low (blue) plant O_3 sensitivities are shown. For the herbaceous PFTs the low sensitivity calibration is separate for Mediterranean regions (black). The solid line is the regression line through the modelled points, the dashed line is the regression line from the observed dose-response relationship.

	High Sensitivity				
	BT	**NT**	**C3**	**C4**	**SH**
F_{O3crit} (nmol/m^2/s)	1.00	1.00	1.00	1.00	1.00
a (mmol/m^2)	0.110	0.030	0.200	0.220	0.130
Function	Birch/Beech: y=100.2-0.93x	Norway spruce: y=99.8-0.22x	Wheat: y=100.3-3.85x	Wheat: y=100.3-3.85x	Birch/Beech: y=100.2-0.93x
dqcrit (kg kg^{-1})	0.09	0.06	0.1	0.075	0.1
f0	0.875	0.875	0.9	0.8	0.9
g_1 (kPa$^{0.5}$)	3.22	2.22	5.56	1.1	2.24
	Low Sensitivity				
	BT	**NT**	**C3**	**C4**	**SH**
F_{O3crit} (nmol/m^2/s)	1.00	1.00	1.00	1.00	1.00
a (mmol/m^2)	0.090	0.020	0.060	0.063	0.100
Function	Birch/Beech: y=100.2-0.74x	Norway spruce: y=99.8-0.17x	Temperate perennial grassland: y=93.9-0.99x	Temperate perennial grassland: y=93.9-0.99x	Birch/Beech: y=100.2-0.74x
	High Sensitivity				
	BT - Med.				
F_{O3crit} (nmol/m^2/s)	1.00				
a (mmol/m^2)	0.040				
Function	Dec. Oaks: y=100.3-0.32x				
	Low Sensitivity				
	BT - Med.	**C3 - Med.**	**C4 - Med.**		
F_{O3crit} (nmol/m^2/s)	1.00	1.00	1.00		
a (mmol/m^2)	0.030	0.050	0.060		
Function	Dec. Oaks: y=100.3-0.22x	Mediterranean annual pasture: y=97.1-0.85x	Mediterranean annual pasture: y=97.1-0.85x		

Table S1. PFT-specific parameter values used in the O_3 uptake and g_s formulation in JULES. F_{O3crit} is the critical O_3 threshold above which damage occurs, *a* determines the reduction in photosynthesis with O_3 exposure, 'function' shows the regression equation for the observed functions (x is F_{O3crit}), dq_{crit} (kg kg^{-1}) is a PFT specific parameters representing the critical humidity deficit at the leaf surface (used in the default JULES g_s model), f_0 is the leaf internal to atmospheric CO_2 ratio (c_i/c_a) at the leaf specific humidity deficit (also used in the default JULES g_s model), and g_1 is the PFT specific parameter of the Medlyn *et al*., (2011) g_s model. The parameters dq_{crit}, f_0 and g_1 vary by PFT, but not by O_3 sensitivity so are only shown once here.

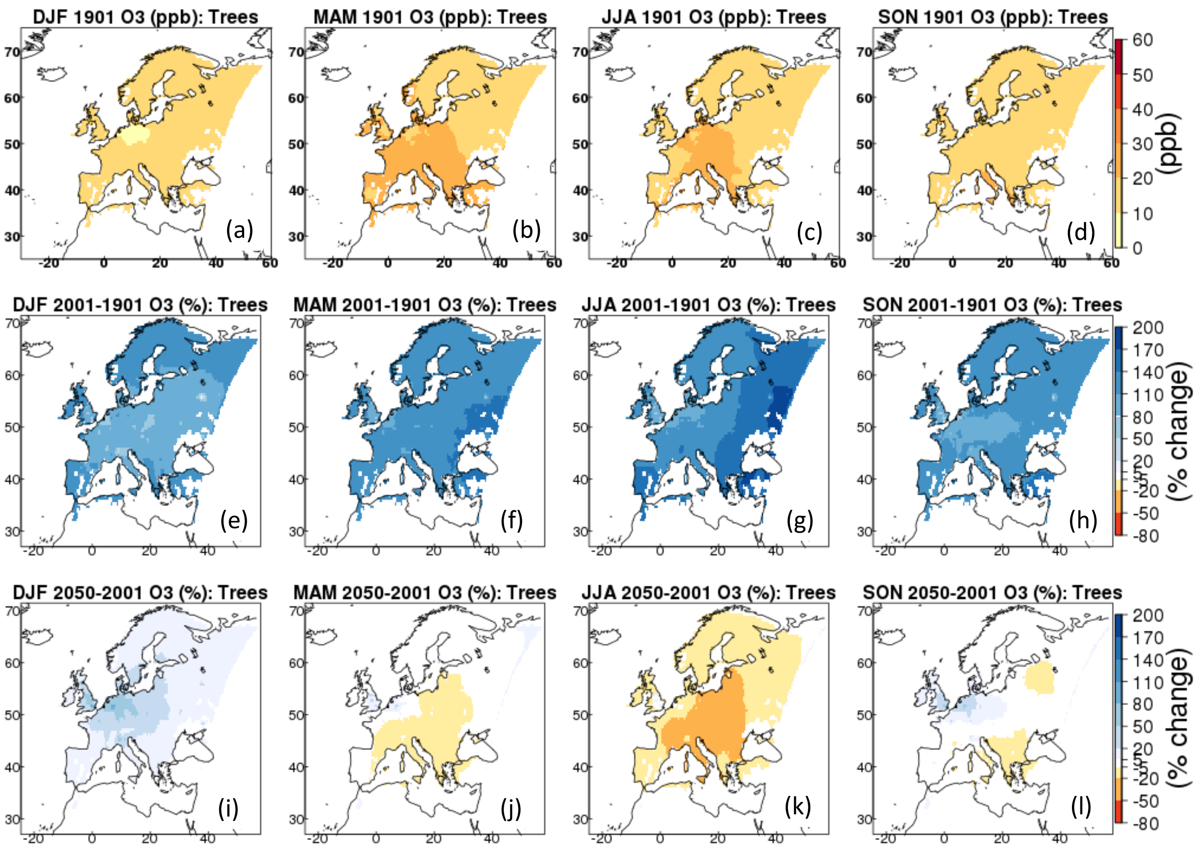

Figure S3. (a-d) 1901 seasonal mean (DJF, MAM, JJA, SON) O_3 concentration (ppb) from EMEP for woody (tree and shrub) PFTs; (e-h) change in seasonal O_3 concentration (%) from 1901 to 2001; (i-l) change in seasonal O_3 concentration (%) from 2001 to 2050.

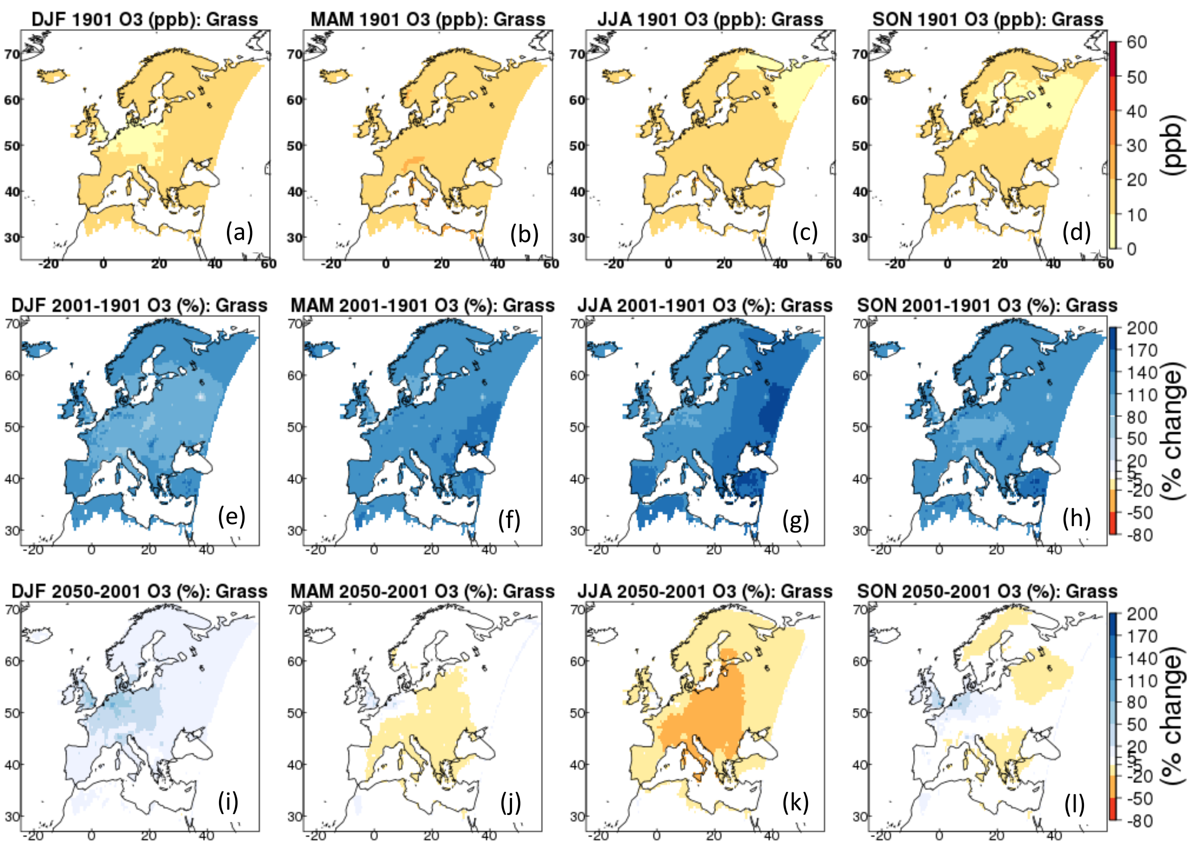

Figure S4. (a-d) 1901 seasonal mean (DJF, MAM, JJA, SON) O_3 concentration (ppb) from EMEP for herbaceous PFTs; (e-h) change in seasonal O_3 concentration (%) from 1901 to 2001; (i-l) change in seasonal O_3 concentration (%) from 2001 to 2050.

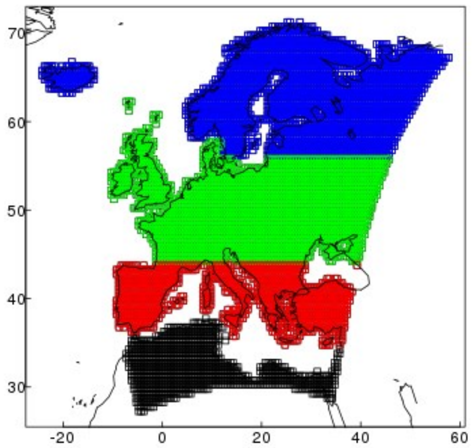

Figure S5. Regions, blue is Boreal, green is Temperate, red is Mediterranean.

S3 Assessing the difference between gs model formulation

Here we assess the impact of g_s model formulation, comparing the standard JULES Jacobs (1994) formulation (equation 6) with the alternative Medlyn *et al*., (2011) formulation (equation 7). This was done for two contrasting grid points (wet/dry) in central Europe with a fixed fractional cover of 20% for each PFT.

JULES was spun-up for 20 years (1979-1999) at two grid points in central Europe representing a wet (lat: 48.25; lon:, 5.25) and a dry site (lat: 38.25; lon:, -7.75). The WFDEI meteorological forcing dataset was used (Weedon, 2013), along with atmospheric CO_2 concentration for the year 1999 (368.33 ppm), and either no O_3 (i.e. the O_3 damage model was switched off) for the control simulations, or spatially explicit fields of present day O_3 concentration produced using the UK Chemistry and Aerosol (UKCA) model from the run evaluated by O'Connor et al. (2014) for the simulations with O_3. Following the spin-up period, JULES was run for one year (2000) with corresponding atmospheric CO_2 concentration, and tropospheric O_3 concentrations as described above. The control and ozone simulations were performed for both *gs* model formulations (Medlyn et al. (2011) and (Jacobs, 1994)). Land cover for the spin-up and main run was fixed at 20% for each PFT. For the simulations including O_3 damage, the high plant O_3 sensitivity parameterisation was used. The difference between these simulations was used to assess the impact of *gs* model formulation on the leaf level fluxes of carbon and water. The modelled soil moisture stress factor (fsmc) at the wet site ranged from 0.8 to 1.0 over the year 2000 (1.0 indicates no soil moisture stress), and at the dry site fsmc steadily declined from 0.8 at the start of the year to 0.25 by the end of the summer.

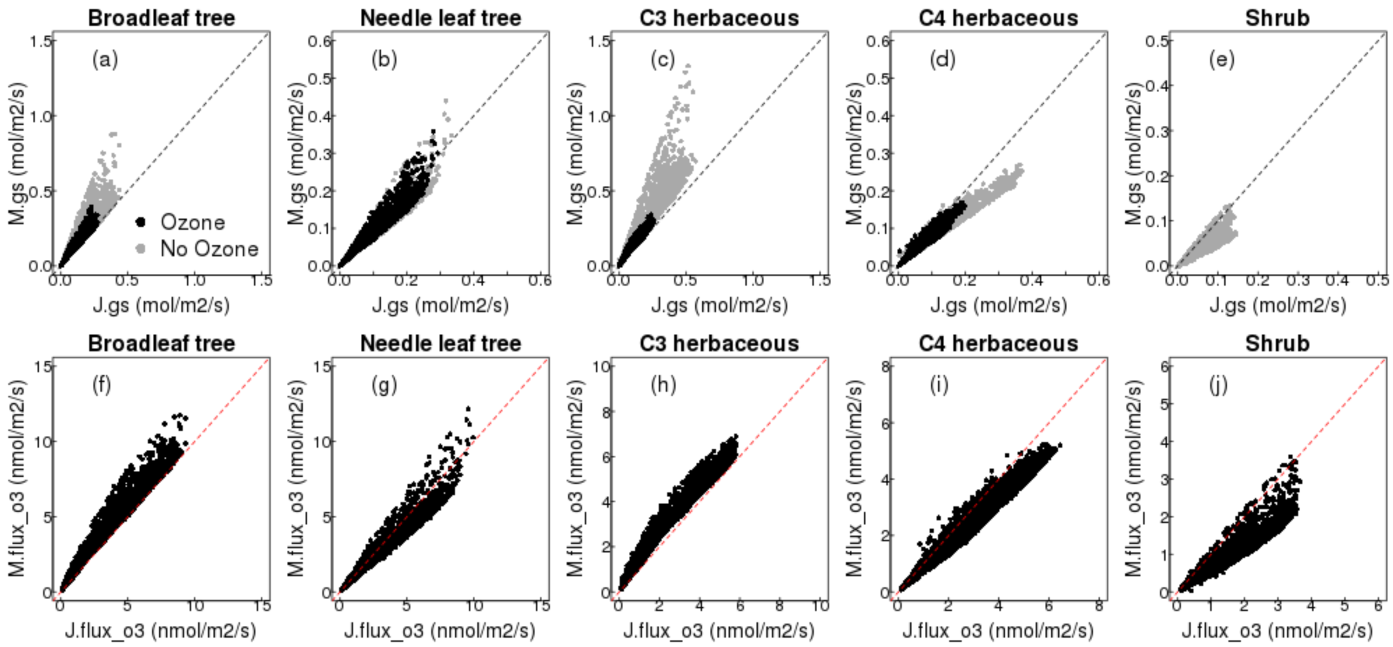

Figure S6. Comparison of the Medlyn *et al*., (2011) g_s model (y axis) versus the Jacobs (1994) g_s model (x axis) currently used in JULES for all five JULES PFTs, for stomatal conductance (*gs*, top row) and the flux of O_3 through the stomata (flux_o3, bottom row) for a dry site.

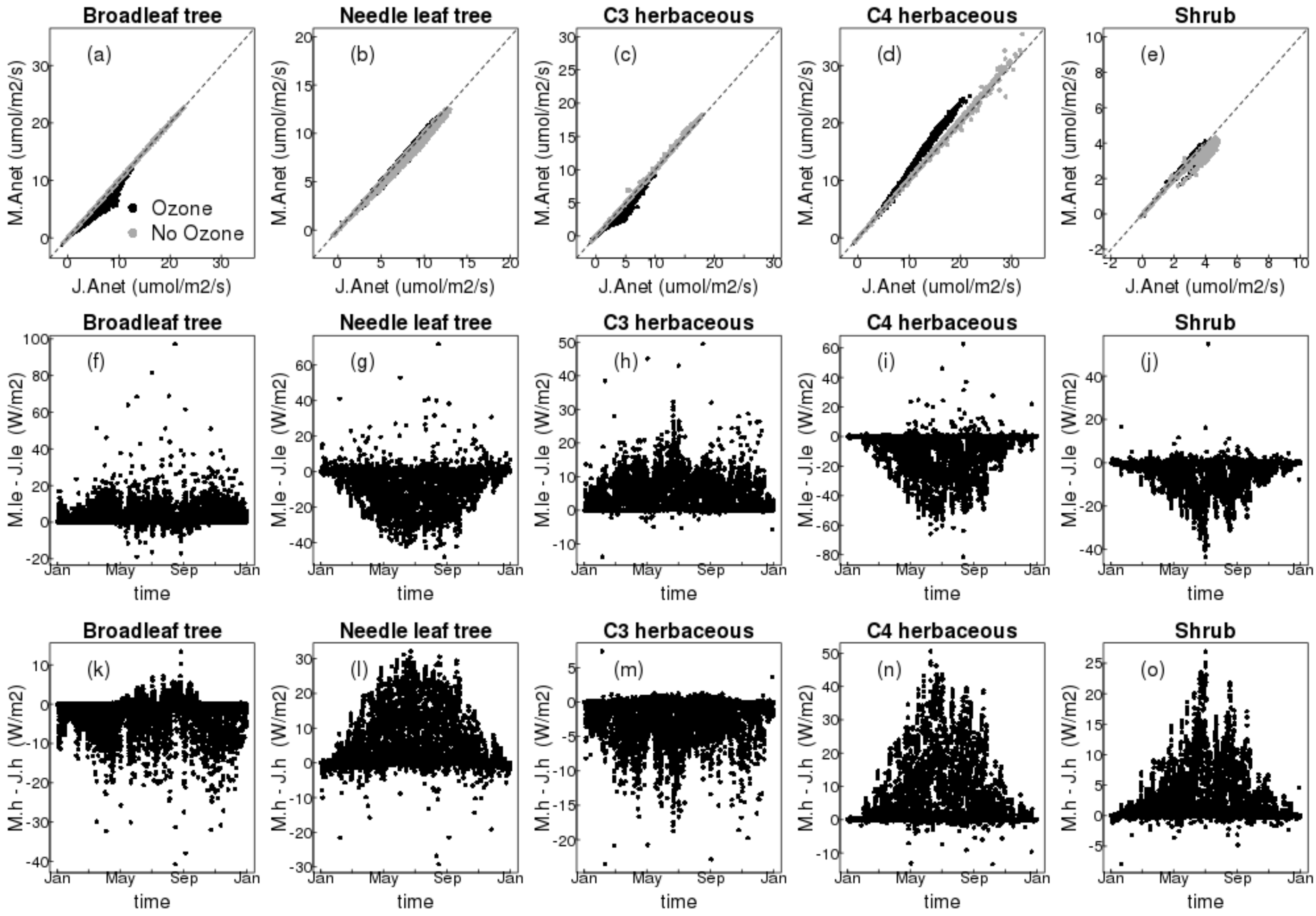

Figure S7. Comparison of the Medlyn *et al*., (2011) g_s model (y axis) versus the Jacobs (1994) g_s model (x axis) currently used in JULES for all five JULES PFTs at a wet site, for net photosynthesis (*Anet*, top row). Residual plots (Medlyn - Jacobs) show the difference between models over the year for latent heat (le, middle row) and sensible heat (h, bottom row).

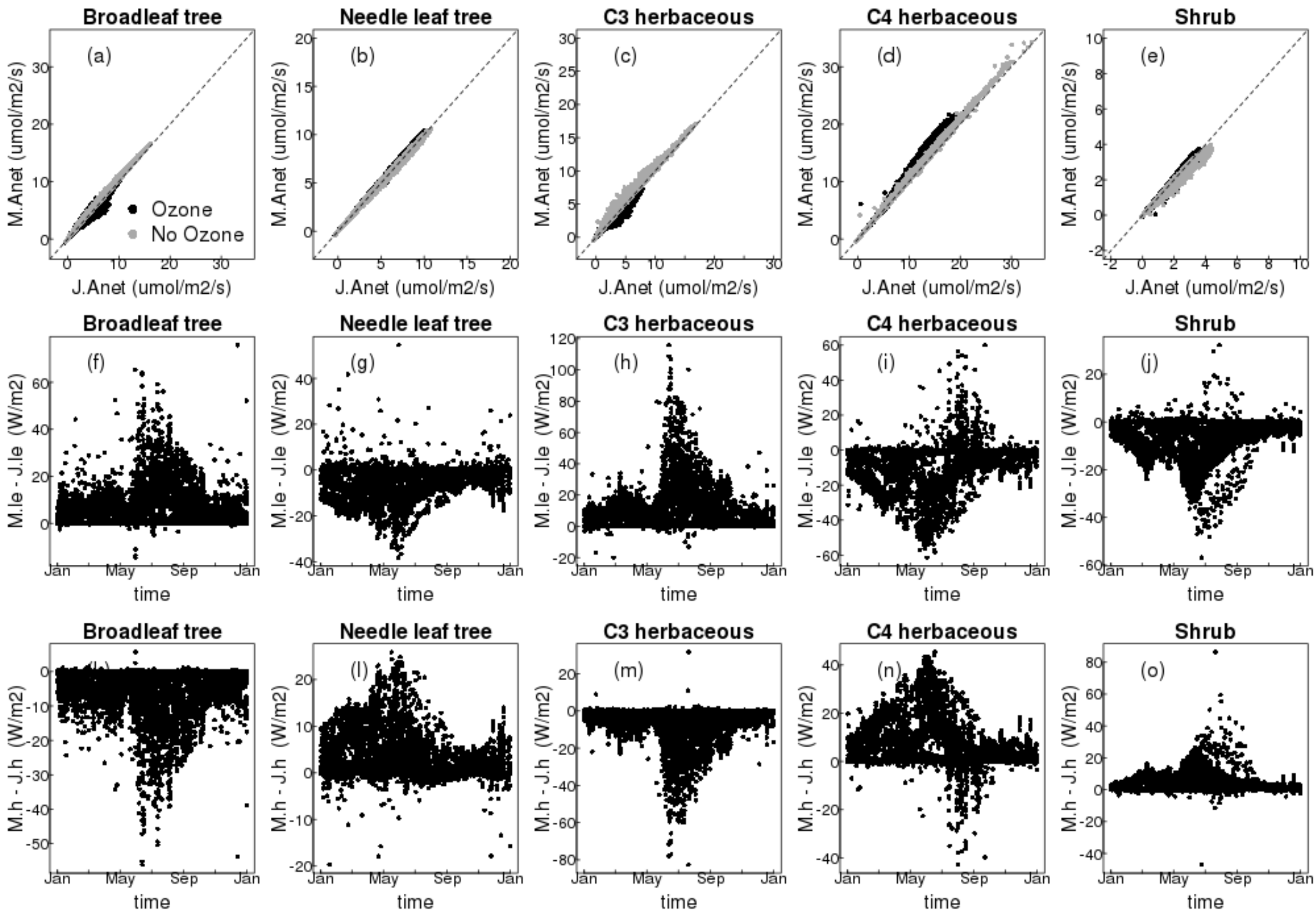

Figure S8. Comparison of the Medlyn *et al*., (2011) g_s model (y axis) versus the Jacobs (1994) g_s model (x axis) currently used in JULES for all five JULES PFTs at a dry site, for net photosynthesis (*Anet*, top row). Residual plots (Medlyn - Jacobs) show the difference between models over the year for latent heat (le, middle row) and sensible heat (h, bottom row).

S4 Estimation of effects due to O_3, CO_2 and O_3 with CO_2

For each variable analysed (GPP, NPP, vegetation carbon, soil carbon, total land carbon and *gs*), we use the mean over 10 years to represent each time period, e.g. the mean over 2040 to 2050 is what we call 2050, 1901 to 1910 is what we refer to as 1901. The difference between the simulations gives the effect of O_3 and CO_2 either separately or in combination over the different time periods. We look at the percentage change due to either O_3 at pre-industrial CO_2 concentration (i.e. without the additional effect of atmospheric CO_2 on stomatal behaviour), CO_2 (at fixed pre-industrial O_3 concentration) or the combined effect of both gases, which is calculated as:

$$100 * (var[y_1] – var[y_2]) / var[y_2] \qquad \text{(S1)}$$

Where $var[y_x]$ represents the variable in time period y, e.g. $100 * (varO_3[2050] – varO_3[1901]) / varO_3[1901]$ gives the O_3 effect (at fixed CO_2) over the full experimental period.

It has been suggested that elevated atmospheric CO_2 provides some protection against plant O_3 damage by reducing *gs* and therefore reducing dry deposition of O_3 through plant stomata (Wittig et al., 2007;Ainsworth et al., 2012). We assess this protection by comparing the O_3 effect at fixed pre-industrial CO_2 concentration (calculated using equation S1 e.g. 100 * ($fixCO_2varO_3$[2050] – $fixCO_2fixO_3$[2050]) / $fixCO_2fixO_3$[2050]) with the O_3 effect produced when CO_2 concentration is increasing, calculated as 100 * ($varCO_2varO_3$[2050] – $varCO_2fixO_3$[2050]) / $varCO_2fixO_3$[2050]. Fix refers to fixed pre-industrial concentration of either gas and var refers to time varying changes in concentration. The difference between these defines the alleviation of the O_3 effect by CO_2. The meteorological forcing is prescribed in these simulations and is therefore the same between the model runs. Other climate factors, such as VPD, temperature and soil moisture availability are accounted for in our simulations, but our analysis isolates the effects of O_3, CO_2 and O_3 + CO_2.

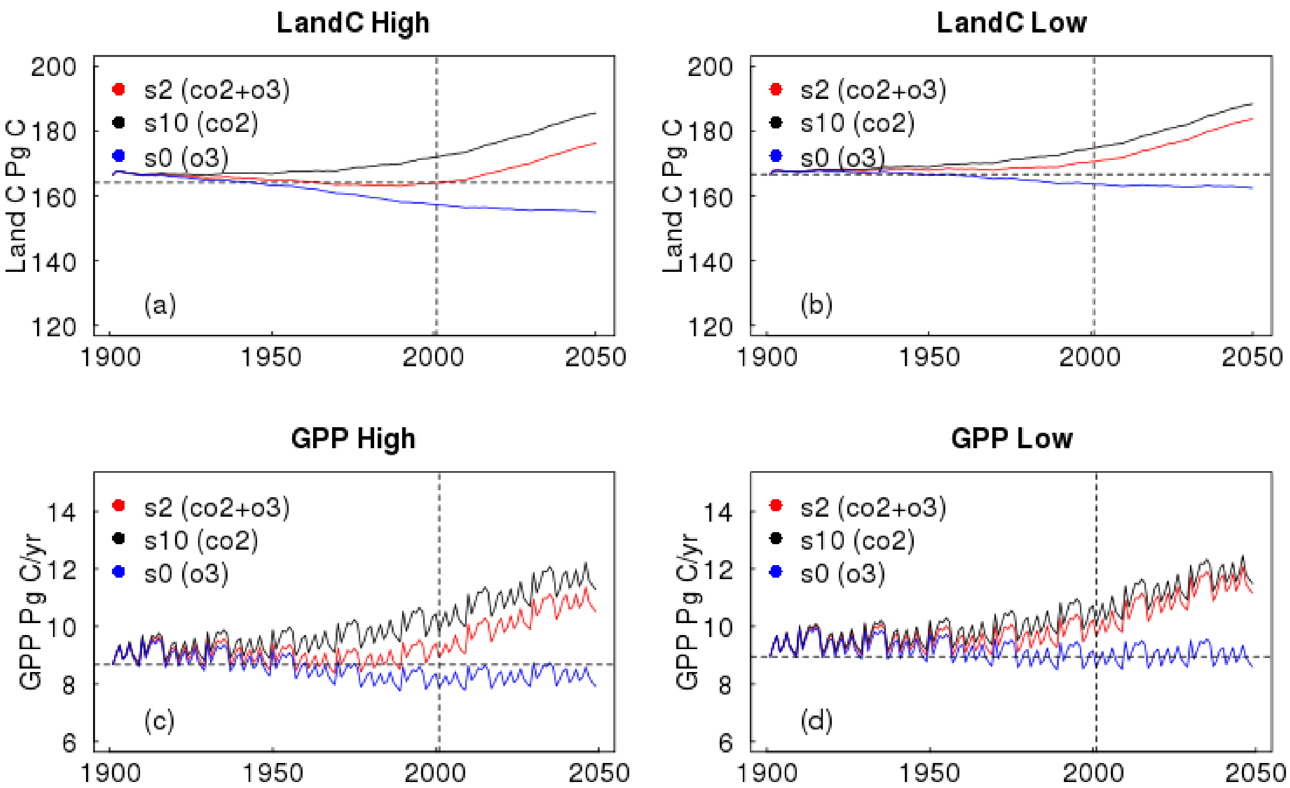

Figure S9. Times series (1901 to 2050) of changes in total carbon stocks (Land C) and gross primary productivity (GPP) due to O_3 effects at fixed pre-industrial atmospheric CO_2 concentration (O_3, blue), CO_2 effects at fixed pre-industrial O_3 concentration (CO_2, black), and effects of CO_2 and O_3 together (CO_2+O_3, red), for the higher and lower plant O_3 sensitivity. The horizontal dashed line shows the pre-industrial value, and the vertical dashed line marks the year 2001.

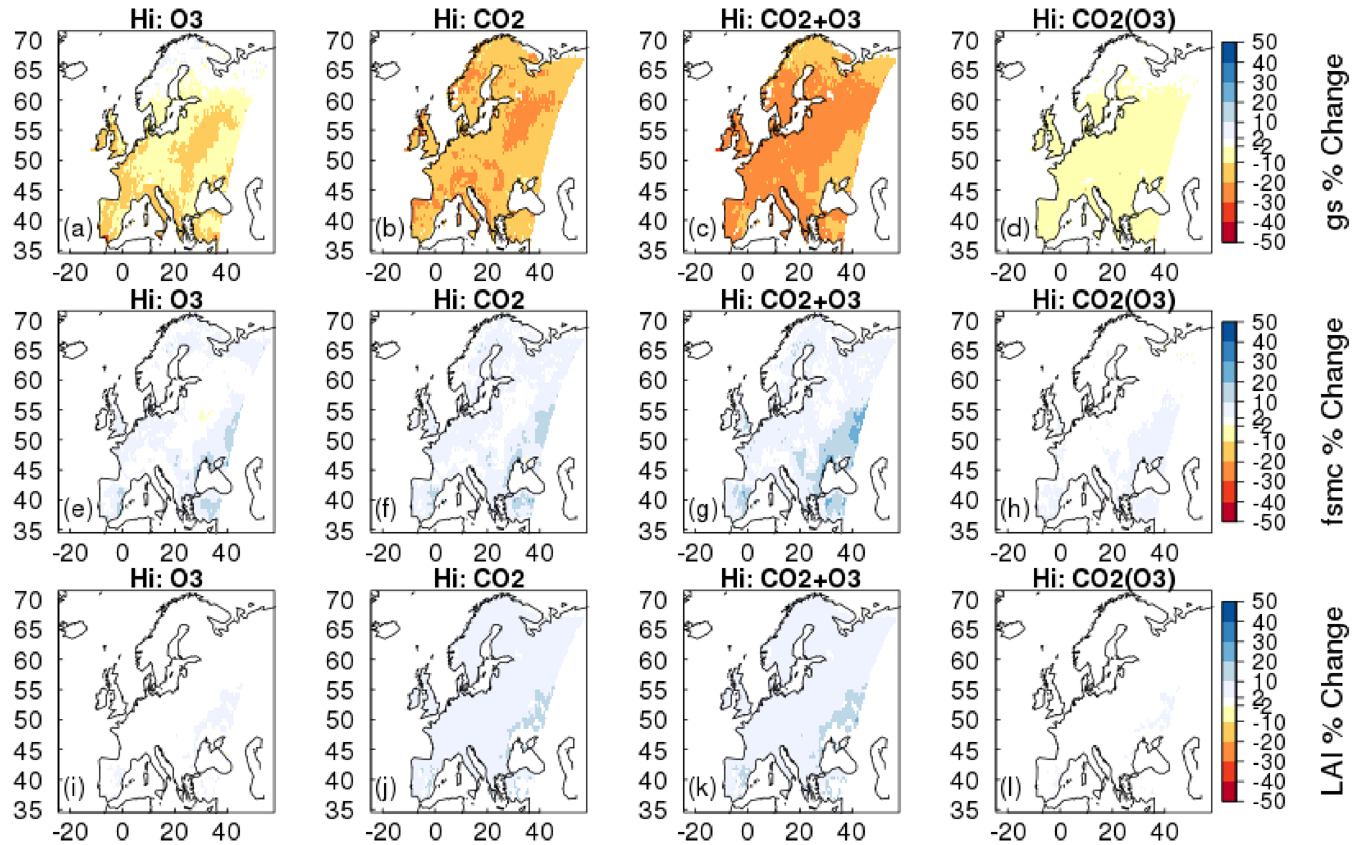

Figure S10. Simulated percentage change in stomatal conductance (gs) a-c), soil moisture availability factor (fsmc) d-e) and leaf area index (*LAI*) g-i) due to O_3 effects at fixed pre-industrial atmospheric CO_2 concentration (O3), CO_2 effects at fixed pre-industrial O_3 concentration (CO2), and effects of CO_2 and O_3 changing simultaneously (CO2+O3). Changes are shown for the periods 1901 to 2050 for the higher plant O_3 sensitivity.

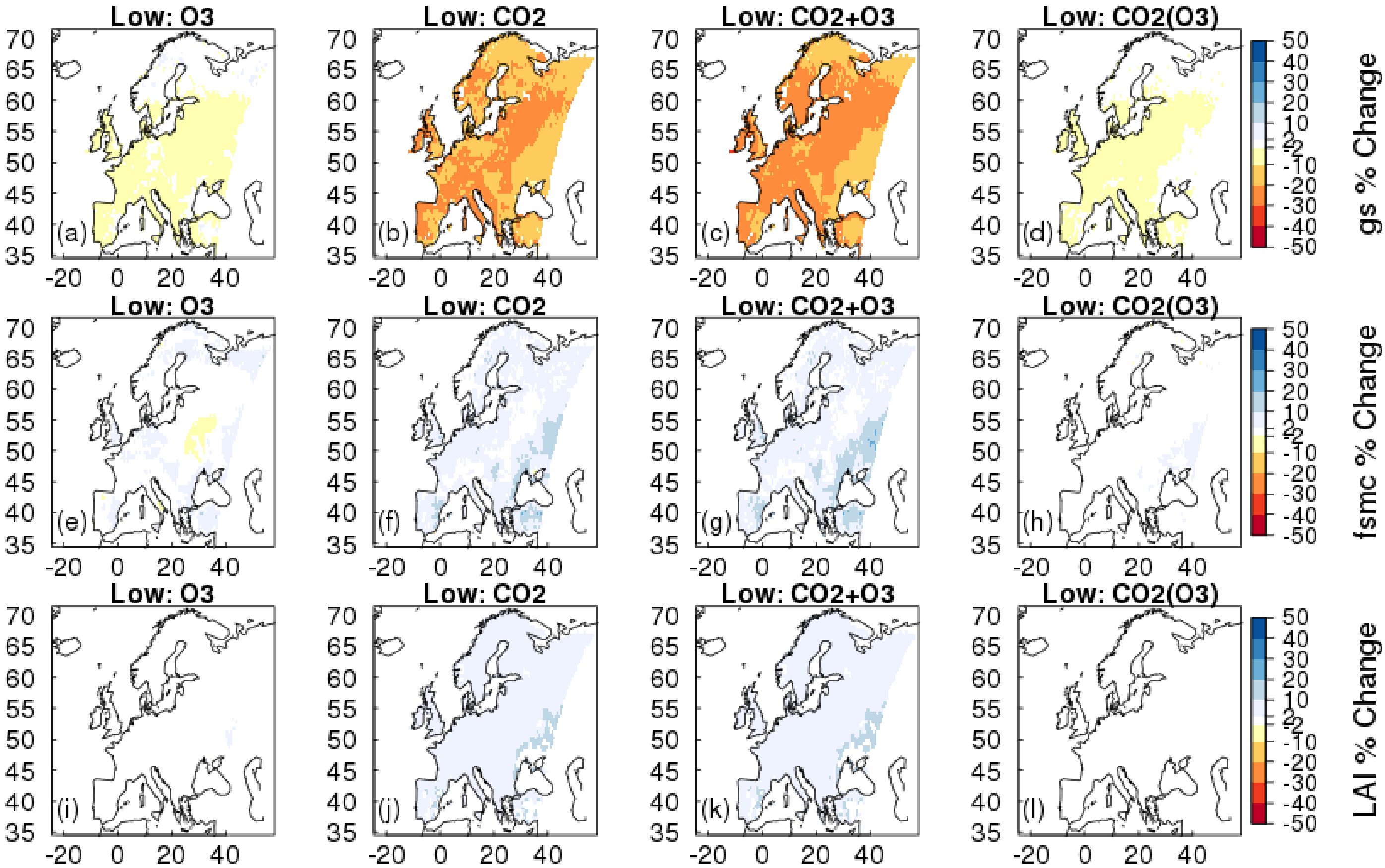

Figure S11. Simulated percentage change in stomatal conductance (gs) a-c), soil moisture availability factor (fsmc) d-e) and leaf area index (*LAI*) g-i) due to O_3 effects at fixed pre-industrial atmospheric CO_2 concentration (O3), CO_2 effects at fixed pre-industrial O_3 concentration (CO2), and effects of CO_2 and O_3 changing simultaneously (CO2+O3). Changes are shown for the periods 1901 to 2050 for the lower plant O_3 sensitivity.

	Future run, constant climate (1901 - 2001)					
	Hi Sensitivity					
	GPP ($Pg\ C\ yr^{-1}$)	NPP ($Pg\ C\ yr^{-1}$)	g_s (m/s)	Veg C (Pg C)	Soil C (Pg C)	Land C (Pg C)
Value in 1901:	9.05	4.46	0.03228	41.1	125.8	167
Absolute diff. (2001 - 1901):						
O_3	-0.81	-0.47	0.00	-0.02	-9.09	-9.21
CO_2	1.16	0.76	0.00	2.82	1.52	4.24
CO_2 + O_3	0.13	0.12	0.00	2.37	-5.55	-3.28
Relative diff. (%)	(%)	(%)	(%)	(%)	(%)	(%)
O_3	-8.95	-10.54	-8.55	-0.05	-7.23	-5.51
CO_2	12.82	17.04	-6.07	6.86	1.21	2.54
CO_2 + O_3	1.44	2.69	-13.66	5.77	-4.41	-1.96
	Lower Sensitivity					
	GPP ($Pg\ C\ yr^{-1}$)	NPP ($Pg\ C\ yr^{-1}$)	g_s (m/s)	Veg C (Pg C)	Soil C (Pg C)	Land C (Pg C)
Value in 1901:	9.34	4.65	0.03319	41.1	126.4	167.5
Absolute diff. (2001 - 1901):						
O_3	-0.30	-0.21	0.00	-0.21	-3.38	-3.59
CO_2	1.15	0.74	0.00	2.73	3.70	6.43
CO_2 + O_3	0.65	0.43	0.00	2.21	0.29	2.50
Relative diff. (%)	(%)	(%)	(%)	(%)	(%)	(%)
O_3	-3.21	-4.52	-3.31	-0.51	-2.67	-2.14
CO_2	12.31	15.91	-6.39	6.64	2.93	3.84
CO_2 + O_3	6.96	9.25	-9.88	5.38	0.23	1.49

Table S2. Simulated changes in the European land carbon cycle due to changing O_3 and CO_2 concentrations. Shown are changes in total carbon stocks (Land C), split into vegetation (Veg C) and soil (Soil C) carbon, and gross primary productivity (GPP), net primary productivity (NPP) and conductance (g_s), between 1901 and 2001.

	Future run, constant climate (2001 - 2050)					
	Hi Sensitivity					
	GPP (Pg C yr^{-1})	NPP (Pg C yr^{-1})	g_s (m/s)	Veg C (Pg C)	Soil C (Pg C)	Land C (Pg C)
Value in 2001:						
O_3	8.24	3.99	0.02952	41.08	116.71	157.79
CO_2	10.21	5.22	0.03032	43.92	127.32	171.24
$CO_2 + O_3$	9.18	4.58	0.02787	43.47	120.25	163.72
Absolute diff. (2050 - 2001):						
O_3	0.01	0.00	0.00	-0.09	-2.35	-2.44
CO_2	1.42	0.95	0.00	5.25	7.73	12.98
$CO_2 + O_3$	1.66	1.07	0.00	5.11	6.00	11.11
Relative diff. (%)	(%)	(%)	(%)	(%)	(%)	(%)
O_3	0.12	0.00	0.00	-0.22	-2.01	-1.55
CO_2	13.91	18.20	-13.89	11.95	6.07	7.58
$CO_2 + O_3$	18.08	23.36	-11.37	11.76	4.99	6.79

	Lower Sensitivity					
	GPP (Pg C yr^{-1})	NPP (Pg C yr^{-1})	g_s (m/s)	Veg C (Pg C)	Soil C (Pg C)	Land C (Pg C)
Value in 2001:						
O_3	9.04	4.44	0.03	40.89	123.02	163.91
CO_2	10.49	5.39	0.03	43.83	130.1	173.93
$CO_2 + O_3$	9.99	5.08	0.02991	43.31	126.69	170
Absolute diff. (2050 - 2001):						
O_3	0.02	-0.06	0.00	-0.13	-0.94	-1.07
CO_2	1.35	0.92	0.00	5.25	7.89	13.14
$CO_2 + O_3$	1.50	1.00	0.00	5.11	7.25	12.35
Relative diff. (%)	(%)	(%)	(%)	(%)	(%)	(%)
O_3	0.22	-1.35	-0.72	-0.32	-0.76	-0.65
CO_2	12.87	17.07	-14.64	11.98	6.06	7.55
$CO_2 + O_3$	15.02	19.69	-13.37	11.80	5.72	7.26

Table S3. Simulated changes in the European land carbon cycle due to changing O_3 and CO_2 concentrations. Shown are changes in total carbon stocks (Land C), split into vegetation (Veg C) and soil (Soil C) carbon, and gross primary productivity (GPP), net primary productivity (NPP) and conductance (g_s), between 2001 and 2050.

	Future run, constant climate (1901 - 2050)					
	Hi Sensitivity					
	GPP (Pg C yr^{-1})	NPP (Pg C yr^{-1})	g_s (m/s)	Veg C (Pg C)	Soil C (Pg C)	Land C (Pg C)
Value in 1901:	9.05	4.46	0.03228	41.1	125.8	167
Absolute diff. (2050 - 1901):						
O_3	-0.80	-0.47	0.00	-0.11	-11.44	-11.65
CO_2	2.58	1.71	-0.01	8.07	9.25	17.22
CO_2 + O_3	1.79	1.19	-0.01	7.48	0.45	7.83
Relative diff. (%)	(%)	(%)	(%)	(%)	(%)	(%)
O_3	-8.84	-10.54	-8.55	-0.27	-9.09	-6.98
CO_2	28.51	38.34	-19.11	19.64	7.35	10.31
CO_2 + O_3	19.78	26.68	-23.48	18.20	0.36	4.69
	Lower Sensitivity					
	GPP (Pg C yr^{-1})	NPP (Pg C yr^{-1})	g_s (m/s)	Veg C (Pg C)	Soil C (Pg C)	Land C (Pg C)
Value in 1901:	9.34	4.65	0.03319	41.1	126.4	167.5
Absolute diff. (2050 - 1901):						
O_3	-0.40	-0.27	0.00	-0.34	-4.32	-4.66
CO_2	2.50	1.66	-0.01	7.98	11.59	19.57
CO_2 + O_3	2.15	1.43	-0.01	7.32	7.54	14.85
Relative diff. (%)	(%)	(%)	(%)	(%)	(%)	(%)
O_3	-4.28	-5.81	-4.01	-0.83	-3.42	-2.78
CO_2	26.77	35.70	-20.10	19.42	9.17	11.68
CO_2 + O_3	23.02	30.75	-21.93	17.81	5.97	8.87

Table S4. Simulated changes in the European land carbon cycle due to changing O_3 and CO_2 concentrations. Shown are changes in total carbon stocks (Land C), split into vegetation (Veg C) and soil (Soil C) carbon, and gross primary productivity (GPP), net primary productivity (NPP) and conductance (g_s), between 1901 and 2050.

	GPP_hi ($Pg\ C\ yr^{-1}$)	GPP_low ($Pg\ C\ yr^{-1}$)	LandC_hi (Pg C)	LandC_low (Pg C)
Value in 1901:	9.05	9.34	167.00	167.50
Value in 2050:				
CO_2	11.63	11.84	184.22	187.07
O_3	8.25	8.94	155.35	162.84
$CO_2 + O_3$	10.84	11.49	174.83	182.35
% change due to O_3 at PI CO_2	-8.84	-4.28	-6.98	-2.78
% change due to O_3 at high CO_2	-6.79	-2.96	-5.10	-2.52
Alleviation of O_3 damage by CO_2 increase (%)	2.05	1.33	1.88	0.26

Table S5. Percentage reduction in simulated GPP and Land C by 2050 due to future O_3 effects at pre-industrial (PI) CO_2 concentration, and under increasing future CO_2 concentration. The difference between these defines the alleviation of the O_3 effect by CO_2.

References

Ainsworth, E. A., Yendrek, C. R., Sitch, S., Collins, W. J., and Emberson, L. D.: The Effects of Tropospheric Ozone on Net Primary Productivity and Implications for Climate Change, Annual Review of Plant Biology, 63, 637-661, doi:10.1146/annurev-arplant-042110-103829, 2012.

Büker, P., Feng, Z., Uddling, J., Briolat, A., Alonso, R., Braun, S., Elvira, S., Gerosa, G., Karlsson, P. E., Le Thiec, D., Marzuoli, R., Mills, G., Oksanen, E., Wieser, G., Wilkinson, M., and Emberson, L. D.: New flux based dose-response relationships for ozone for European forest tree species, Environmental Pollution, 163-174, 2015.

CLRTAP: The UNECE Convention on Long-range Transboundary Air Pollution. Manual on Methodologies and Criteria for Modelling and Mapping Critical Loads and Levels and Air Pollution Effects, Risks and Trends: Chapter III Mapping Critical Levels for Vegetation, accessed via, http://icpvegetation.ceh.ac.uk/publications/documents/Chapter3-Mappingcriticallevelsforvegetation_000.pdf, 2017.

IGBP-DIS: International Geosphere-Biosphere Programme, Data and Information System, Potsdam, Germany. Available from Oak Ridge National Laboratory Distributed Active Archive Center, Oak Ridge, TN, ailable at: http://www.daac.ornl.gov,

Jacobs, C. M. J.: Direct impact of atmospheric CO_2 enrichment on regional transpiration, Wageningen Agricultural University, 1994.

Karlsson, P. E., Braun, S., Broadmeadow, M., Elvira, S., Emberson, L., Gimeno, B. S., Le Thiec, D., Novak, K., Oksanen, E., Schaub, M., Uddling, J., and Wilkinson, M.: Risk assessments for forest trees: The performance of the ozone flux versus the AOT concepts, Environmental Pollution, 146, 608-616, http://dx.doi.org/10.1016/j.envpol.2006.06.012, 2007.

Medlyn, B. E., Duursma, R. A., Eamus, D., Ellsworth, D. S., Prentice, I. C., Barton, C. V., Crous, K. Y., de Angelis, P., Freeman, M., and Wingate, L.: Reconciling the optimal and empirical approaches to modelling stomatal conductance, Global Change Biology, 17, 2134-2144, 2011.

O'Connor, F. M., Johnson, C. E., Morgenstern, O., Abraham, N. L., Braesicke, P., Dalvi, M., Folberth, G. A., Sanderson, M. G., Telford, P. J., Voulgarakis, A., Young, P. J., Zeng, G., Collins, W. J., and Pyle, J. A.: Evaluation of the new UKCA climate-composition model – Part 2: The Troposphere, Geosci. Model Dev., 7, 41-91, 10.5194/gmd-7-41-2014, 2014.

Tans, P., and Keeling, R.: Dr. Pieter Tans, NOAA/ESRL (www.esrl.noaa.gov/gmd/ccgg/trends/) and Dr. Ralph Keeling, Scripps Institution of Oceanography (scrippsco2.ucsd.edu/).

Weedon, G. P.: Readme file for the "WFDEI" dataset.available at: http://www.eu-watch.org/gfx_content/documents/README-WFDEI.pdf, 2013.

Wittig, V. E., Ainsworth, E. A., and Long, S. P.: To what extent do current and projected increases in surface ozone affect photosynthesis and stomatal conductance of trees? A meta-analytic review of the last 3 decades of experiments, Plant, Cell & Environment, 30, 1150-1162, 10.1111/j.1365-3040.2007.01717.x, 2007.